

# Resistance mechanisms and clonal dynamics in mantle cell lymphoma treated with sequential BTKi and venetoclax therapy

Tamás László<sup>1,2</sup> , László Imre Pinczés<sup>3,4</sup>, Bence Báta<sup>1,2,5</sup>, Luca Varga<sup>1,2</sup>, Botond Timár<sup>1,2</sup>, Anita Gulyás<sup>3,4</sup>, Ilona Tárkányi<sup>5</sup>, Márk Plander<sup>6</sup>, Zsolt Nagy<sup>5</sup>, Péter Rajnics<sup>7</sup>, Miklós Egyed<sup>7</sup>, Zsuzsa Molnár<sup>8</sup>, János Rottek<sup>8</sup>, András Masszi<sup>8</sup>, Péter Tamáska<sup>9</sup>, Róbert Szász<sup>3,4</sup>, Árpád Illés<sup>3,4</sup>, Donát Alpár<sup>1,2</sup>, Ferenc Magyar<sup>3,4\*†</sup> and Csaba Bödör<sup>1,2\*†</sup> 

<sup>1</sup> HCEMM-SE Molecular Oncohematology Research Group, Department of Pathology and Experimental Cancer Research, Semmelweis University, Budapest, Hungary

<sup>2</sup> MTA-SE Lendület Molecular Oncohematology Research Group, Department of Pathology and Experimental Cancer Research, Semmelweis University, Budapest, Hungary

<sup>3</sup> Division of Hematology, Department of Internal Medicine, Faculty of Medicine, University of Debrecen, Debrecen, Hungary

<sup>4</sup> Doctoral School of Clinical Medicine, University of Debrecen, Debrecen, Hungary

<sup>5</sup> Department of Internal Medicine and Hematology, Semmelweis University, Budapest, Hungary

<sup>6</sup> Markusovszky University Teaching Hospital, Szombathely, Hungary

<sup>7</sup> Kaposi Mór University Teaching Hospital of County Somogy, Kaposvár, Hungary

<sup>8</sup> National Institute of Oncology, Budapest, Hungary

<sup>9</sup> Borsod-Abaúj-Zemplén County Hospital and University Teaching Hospital, Miskolc, Hungary

\*Correspondence to: C Bödör, Semmelweis University, Department of Pathology and Experimental Cancer Research, H-1085 Budapest, Üllői út 26, Hungary. E-mail: [bodor.csaba@semmelweis.hu](mailto:bodor.csaba@semmelweis.hu); F Magyar, Division of Hematology, Department of Internal Medicine, Faculty of Medicine, University of Debrecen, Nagyerdei korut 98, H-4032 Debrecen, Hungary. E-mail: [magyari.ferenc@med.unideb.hu](mailto:magyari.ferenc@med.unideb.hu)

†These authors are joint senior authors.

## Abstract

In recent years, targeted therapies have become the standard of care for refractory/relapsed mantle cell lymphoma (MCL). Although the mutational profile of MCL has been extensively studied, there is a lack of understanding of resistance mechanisms and genetic factors that impact the response to novel treatments. Since patients relapsing on targeted treatment experience poor clinical outcomes, understanding the genetic foundation of resistance mechanisms in MCL is essential. In this study, we aimed to scrutinize the copy number profile and clonal dynamics of double-resistant MCL patients treated sequentially with Bruton's tyrosine kinase inhibitor (BTKi) and venetoclax using low-coverage whole genome sequencing (lcWGS). Samples obtained after systemic therapy showed more copy number alterations (CNAs) ( $p = 0.039$ ; Wilcoxon) compared to samples collected before treatment initiation. Patients showing early progression on BTKi demonstrated CNAs affecting cytobands encompassing the coding regions of *NOTCH1*, *TRAF2*, *BIRC2*, *BIRC3*, and *ATM*. A deletion in chromosome 9p21.3 was identified in two out of three venetoclax-resistant patients. For patient MCL2, progressing on ibrutinib but showing venetoclax resistance, a 9p21.3 deletion was found throughout the disease course, with acquired *SMARCA4*-del(19)(p13.3-q13.11) and *DLC1*-del(8)(p23.2-q11.1) observed at relapse, highlighting their role in disease progression and therapy resistance. Using lcWGS, an innovative genome-wide approach, this study revealed novel putative primary and acquired resistance mechanisms in BTKi and venetoclax double-resistant MCL patients.

© 2025 The Author(s). *The Journal of Pathology* published by John Wiley & Sons Ltd on behalf of The Pathological Society of Great Britain and Ireland.

**Keywords:** ibrutinib resistance; mantle cell lymphoma; next-generation sequencing; targeted therapy; venetoclax resistance

Received 7 January 2025; Revised 3 March 2025; Accepted 31 March 2025

No conflicts of interest were declared.

## Introduction

Mantle cell lymphoma (MCL) represents a rare subtype of non-Hodgkin lymphomas with remarkable molecular and clinical heterogeneity. Although significant improvements have been made in recent years, relapse or progression

after induction treatment is almost inevitable, with worsening overall survival (OS) and progression-free survival (PFS) after each line of treatment [1]. Recently, targeted therapies including Bruton's tyrosine kinase inhibitor (BTKi) ibrutinib and acalabrutinib have become the cornerstone of treatment in the refractory/relapsed

setting [2–7]. Despite its remarkable clinical effectiveness, primary or acquired resistance to BTKi therapy develops, commonly conferring poor outcomes [8]. Venetoclax, an orally bioavailable proapoptotic BCL2-inhibitor has also shown promising clinical activity in BTKi-resistant patients [9–11]. Although venetoclax offers these patients a viable alternative, like BTKi, venetoclax resistance can also develop leading to a very unfavorable prognosis in this so-called double-resistant patient group [10].

Although the mutational profile of MCL has been extensively studied, there is a lack of understanding regarding resistance mechanisms and genetic factors impacting the response to novel treatment modalities [12,13]. Resistance mutations for targeted therapies involving *BTK* (ibrutinib, acalabrutinib) or *BCL2* (venetoclax) genes are well characterized in chronic lymphocytic leukemia, though they are infrequently observed in MCL [10,14–16]. Currently, it is believed that resistance to ibrutinib develops via abnormal activation of the PI3K-AKT pathway and/or traditional or alternative NFκB pathways, as well as metabolic reprogramming [14,17–19]. However, several of these findings were not verified in independent studies, and the molecular background underlying ibrutinib resistance remains to be investigated. Indeed, only a handful of venetoclax-resistant patients have available molecular data, hence the genetic background of venetoclax resistance remains underexplored [10,20,21]. Previous studies demonstrated that acquisition of mutations in *SMARCA4*, *CARD11*, and *TRAF2* or alterations affecting the SWI-SNF chromatin-remodeling complex might play a role in venetoclax resistance [10,20,21]. Given the poor clinical outcomes in double-resistant patients, improved understanding of resistance mechanisms and clonal dynamics is essential.

Low-coverage whole genome sequencing (lcWGS) is a robust method allowing for comprehensive detection of copy number alterations (CNAs) throughout the entire genome, and can also be applied to DNA extracted from formalin-fixed paraffin-embedded (FFPE) specimens [22]. Considering that peripheral blood is less affected in classical MCL patients, this NGS-based advanced technique offers an important, viable and cost-effective approach for the molecular analysis of malignant tissue samples.

In this study, we aimed to study the changes in copy number profile of MCL patients treated sequentially with BTKi and venetoclax using lcWGS, specifically focusing on double resistant cases. By genome-wide profiling of serial tumor samples, our objective was to enhance the understanding of clonal dynamics and possible resistance mechanisms underlying ibrutinib and venetoclax resistance in MCL.

## Materials and methods

### Ethics approval

The study was approved by the Hungarian Medical Research Council (ID: TUKÉB: IV/5495-3/2021/EKU)

and was conducted in accordance with the Declaration of Helsinki. All patients gave informed consent for the research use of archival tissue material and clinical data.

### Patient characteristics

Twelve patients diagnosed with MCL between 2008 and 2020 were included in this retrospective study. Median age at diagnosis was 66 years (range: 55–80 years), with a female/male ratio of 0.5 (4:8). The majority of patients displayed an advanced stage of disease, with 83% (10/12) classified as having Ann Arbor stage 4 disease [23,24]. Stage 2 and Stage 3 disease were identified in one case each, and no patients were found to have stage 1 disease. In addition, more than half of the patients (58%; 7/12) exhibited high-risk disease, as determined by the Mantle Cell Lymphoma International Prognostic Index (MIPI). Detailed patient characteristics are presented in Supplementary materials and methods, supplementary material, Table S1.

### Patient samples

In this real-world study, 21 formalin-fixed paraffin-embedded (FFPE) tissue samples were analyzed, including those obtained from bone marrow (38%, 8/21), lymph node (24%, 5/21), colon (14%, 3/21), stomach (10%, 2/21), or other sites (14%, 3/21) (supplementary material, Table S2). An expert hematopathologist (BT) performed morphological reevaluation of all samples and assessed the extent of tumor invasion. Tumor samples with less than 20% tumor content were excluded, leading to a median tumor infiltration rate of 80% (range: 20%–90%). DNA was extracted using the QIAamp DNA FFPE Tissue Kit (Qiagen, Hilden, Germany) and quantified with Qubit HS dsDNA Kit (Thermo Fisher Scientific, Waltham, MA, USA).

### Tumor protein 53 (TP53) sequencing

Tumor protein 53 (*TP53*) mutation screening was performed on diagnostic samples using next-generation sequencing (NGS). If diagnostic FFPE material was unavailable or the sequencing was unsuccessful, samples collected prior to targeted treatment initiation were analyzed ( $n = 2$ ). Targeted NGS was performed using the CleanPlex *TP53* panel (Paragon Genomics, CA, USA). Libraries were prepared following the manufacturer's protocols and sequenced on a Miseq platform using V2 chemistry in a micro flow cell with a 300-cycle paired-end configuration. Data processing and analysis were performed as previously described [25]. A detailed description of the *TP53* clinicopathological patient characteristics are available in Supplementary materials and methods, supplementary material, Table S2.

### Immunoglobulin heavy chain gene sequencing

Immunoglobulin heavy chain (IGH) gene rearrangement and somatic hypermutation analyses were carried out as described by Agathangelidis *et al* using consensus *IGH*

gene-specific 3' primers as well as subgroup-specific FR1 or FR2 primers [26]. DNA amplification with FR1/FR2 primers was performed by Sanger sequencing, and the data were analyzed utilizing IMGT V-QUEST, in accordance with the most recent European Research Initiative on CLL recommendations [27]. A detailed description of the immunoglobulin heavy chain variable (IGHV) clinicopathological patient characteristics is presented in Supplementary materials and methods, supplementary material, Table S2.

### Low-coverage whole genome sequencing

The integrity of isolated DNA was assessed using a multiplex GAPDH PCR method as described by van Beers *et al* [28]. DNA damage generated by formalin fixation was repaired utilizing the NEBNext FFPE DNA Repair Kit (New England Biolabs, Ipswich, MA, USA). NGS libraries were constructed using the NEBNext Ultra II DNA Library Prep Kit for Illumina along with NEBNext Unique Dual Index UMI Adaptors (New England Biolabs). During library preparation, samples exhibiting low integrity underwent amplification with two additional PCR cycles. Individual libraries were pooled equimolarly and sequenced on a NextSeq2000 (Illumina, San Diego, CA, USA) instrument using P2 or P3 flow cell with 50-cycle single-read chemistry. Processing and analysis of raw sequencing data were carried out as previously described by our group [29].

## Results

### Clinical outcomes

Prior to targeted therapy, 66% of patients received either a combination of rituximab and bendamustine (four out of 12 patients) or a combination of rituximab, cyclophosphamide, doxorubicin, vincristine, and prednisolone (four out of 12 patients). Additionally, 17% (two out of 12) of patients were treated with rituximab, cyclophosphamide, vincristine, and prednisolone. One patient received treatment according to the NORDIC protocol, and one patient received a single cycle of cyclophosphamide, dexamethasone, and bendamustine for tumor debulking [30]. Conventional treatment modalities were administered prior to the start of BTKi therapy, with a median duration of 11 months (range: 1–82 months). All patients underwent covalent BTKi therapy, with the majority ( $n = 11$ ) receiving ibrutinib and one patient (MCL7) receiving acalabrutinib. The median time to progression on BTKi therapy was 20.5 months (average 23.2 months), ranging from 2 to 87 months (Figure 1). After experiencing progression on BTKi treatment, patients were treated with venetoclax. The average time interval between BTKi progression and initiation of venetoclax treatment was 29.9 days. Venetoclax was administered either as a monotherapy (eight out of 12 patients, 67%) or in combination with other agents (four out of 12 patients, 33%; supplementary material,

Table S1). Following a median duration of 20 months from the initiation of venetoclax treatment, disease progression was observed in 58% (seven out of 12) of patients. Of these seven patients, five succumbed to their disease within a median period of 24 days (Figure 1).

### Evaluation of copy number alterations (CNAs)

LcWGS was used in 21 samples to assess the genome-wide copy number profile of sequential MCL samples (supplementary material, Table S3). Virtually all samples carried at least two arm-level CNAs (range: 2–21). The frequency of deletions was higher, affecting over 90.5% of the samples (19 out of 21), with a median of four deletions per sample (Figure 2, supplementary material, Figure S1). In contrast, arm-level gains were observed in 71.4% (15 out of 21) of samples, with a median of one amplification per sample. Considering arm-level alterations present in at least one-quarter of samples (5/21), deletions most frequently affected the 11q (24%), 13q (67%), 17p(24%), 3p (29%), 6q (48%), 9p (38%), and 9q (48%) chromosome arms, while only the 7p arm was affected by amplifications (38%).

Considering every sample, amplifications were detected in 32% (970 of 3,032) of altered cytobands, while deletions were observed in 67.9% (2,059 of 3,032) of altered cytobands (Figure 2, supplementary material, Figure S1). Three patients were found to carry complex alterations affecting 10p15.2, 13q22.2, and 13q31.3. Several cytobands were affected in more than 50% of samples containing genes previously described to be altered in MCL: 1p21.2 (*SIPRI*), 1p21.1 (*COL11A1*), 6q25.3 (*ARID1B*), 11q22.2 (*BIRC2*, *BIRC3*), 11q22.3 (*ATM*), 13q13.1 (*BRCA2*), 13q14.2 (*FNDC3A*, *RBI*), 13q21.33 (*DIS3*), and 13q31.2 (*SLITRK5*). Of these nine cytobands, six were affected exclusively by deletions, while three exhibited both deletions and amplifications, with deletions being the predominant alterations.

### Comparison of BTKi early versus late progressor patients

We divided the cohort into BTKi early progressors and late progressors based on time to progression, calculated as the time from the start of BTKi treatment to the first time noted for progression. Patients were considered early progressors if they showed clinical signs of progression within a year (range: 2–7 months). For comparison, samples obtained at the time of diagnosis were included. Where diagnostic material was not available, samples collected prior to initiation of targeted treatment were analyzed ( $n = 2$ ). Patients who exhibited early progression on BTKi treatment had a median of one line of prior therapy, compared to a median of two lines of therapy, including radiation therapy, in the 'late progressor' group (supplementary material, Table S1).

Considering arm-level changes, a median of four (average 5.4) alterations were observed in early progressor patients ( $n = 5$ ) versus a median of three (average 3.5) arm-level alterations in late progressors

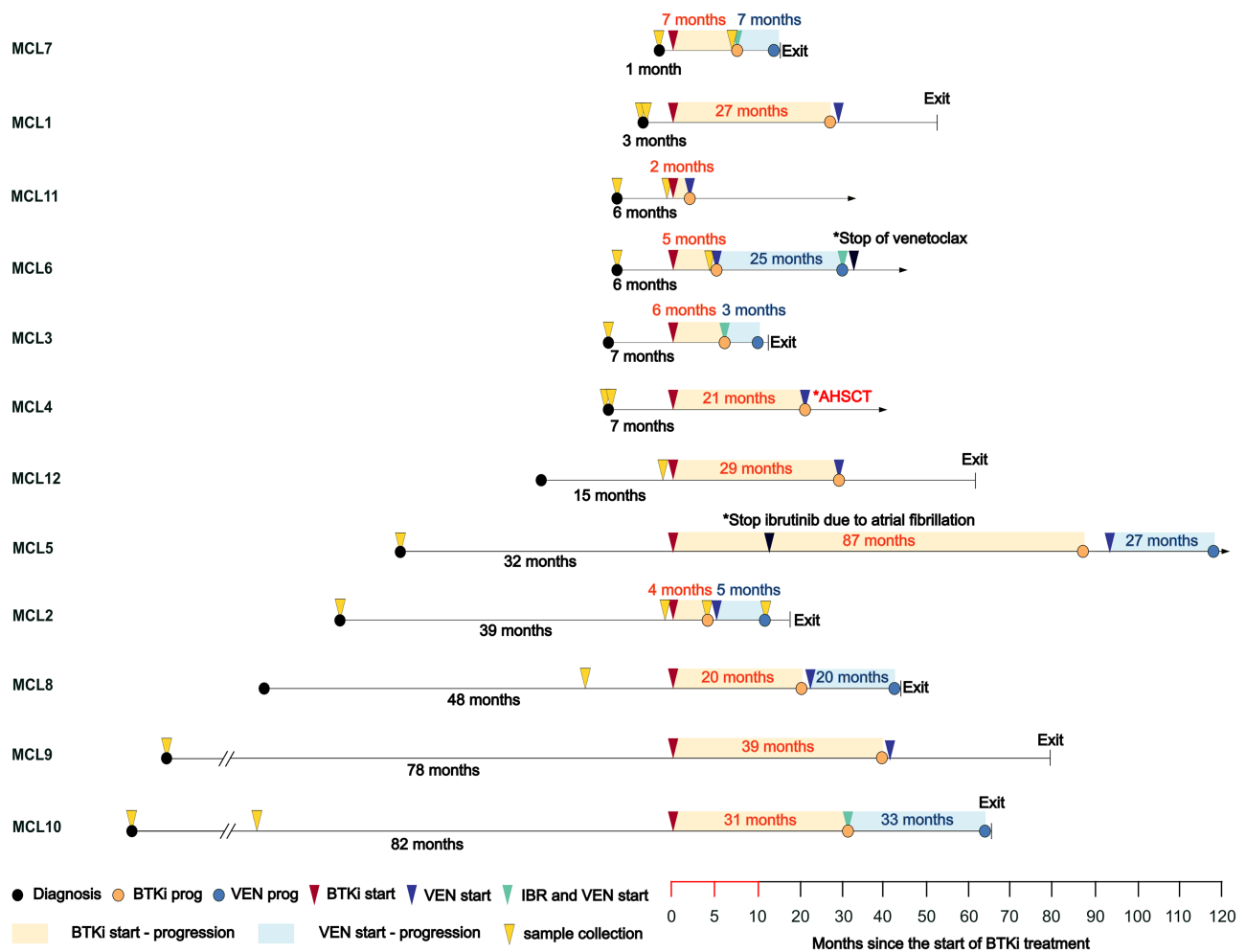


Figure 1. Timeline and main clinical features of MCL patients. Triangles without borders represent the start of a treatment (therapeutic courses prior to the introduction of the initial targeted therapy are not depicted). The yellow triangle with a black border indicates the time of sample collection. The time point of relapse for a particular treatment is represented by circles. Bars between the triangles and circles represent the duration (in months) from the start of a particular treatment to the occurrence of a relapse. The interval between time of diagnosis and onset of BTKi treatment is presented below the cases (in months). Abbreviations: BTKi, Bruton's tyrosine kinase inhibitor; VEN, venetoclax; prog, progression.

( $n = 7$ ). Arm-level deletions affecting the long arm of chromosome 6 were detected in four out of seven patients in the late progressor cohort, whereas this alteration appeared in only one case among early progressors. In the early progressor group ( $n = 5$ ), the most commonly affected cytobands ( $n = 3$  cases) were 1p21.2, 9q34.3, 11q14.2, 11q14.3, 11q22.2, 11q22.3, and 13q14.2 spanning the coding regions of genes previously described to have a potential effect on ibrutinib resistance, such as *NOTCH1*, *TRAF2*, *BIRC2*, *BIRC3*, or *ATM*. Of these cytobands, 1p21.2 (*SIPRI*) and 13q14.2 (*FNDC3A*) were affected exclusively by deletions (Table 1). CNAs affecting cytobands 9q34.3 (*NOTCH1*, *TRAF2*) and 11q14.2 were present only in the early progressor group. Patient MCL2 exhibited deletions at 9q34.3 and 11q14.2, while patients MCL3 and MCL6 displayed isolated deletions at 9q34.3 and 11q14.2, respectively. Patient MCL7 had amplification at both 9q34.3 and 11q14.2 loci. Deletions affecting the long arm of chromosome 13 were identified comparably

in the early and late progressor group (three out of five early progressor versus five out of seven late progressor), highlighting that, despite its high prevalence, its contribution to ibrutinib resistance is unlikely (Figure 2).

#### Comparison of venetoclax responder versus nonresponder patients

Our cohort consisted of nine venetoclax responder and three nonresponder patients. Two out of three nonresponder patients experienced total deletion of chromosome 9, whereas this alteration appeared in only one case (one out of nine) in the responder group. In both cases with del(9p), the extent of the deletion encompassed the coding region of *CDKN2A*. In addition to the total deletion being present in only one responder case (MCL4), deletion of 9p21.3 (*CDKN2A*) was observed in one additional case (MCL9) in the responder cohort.

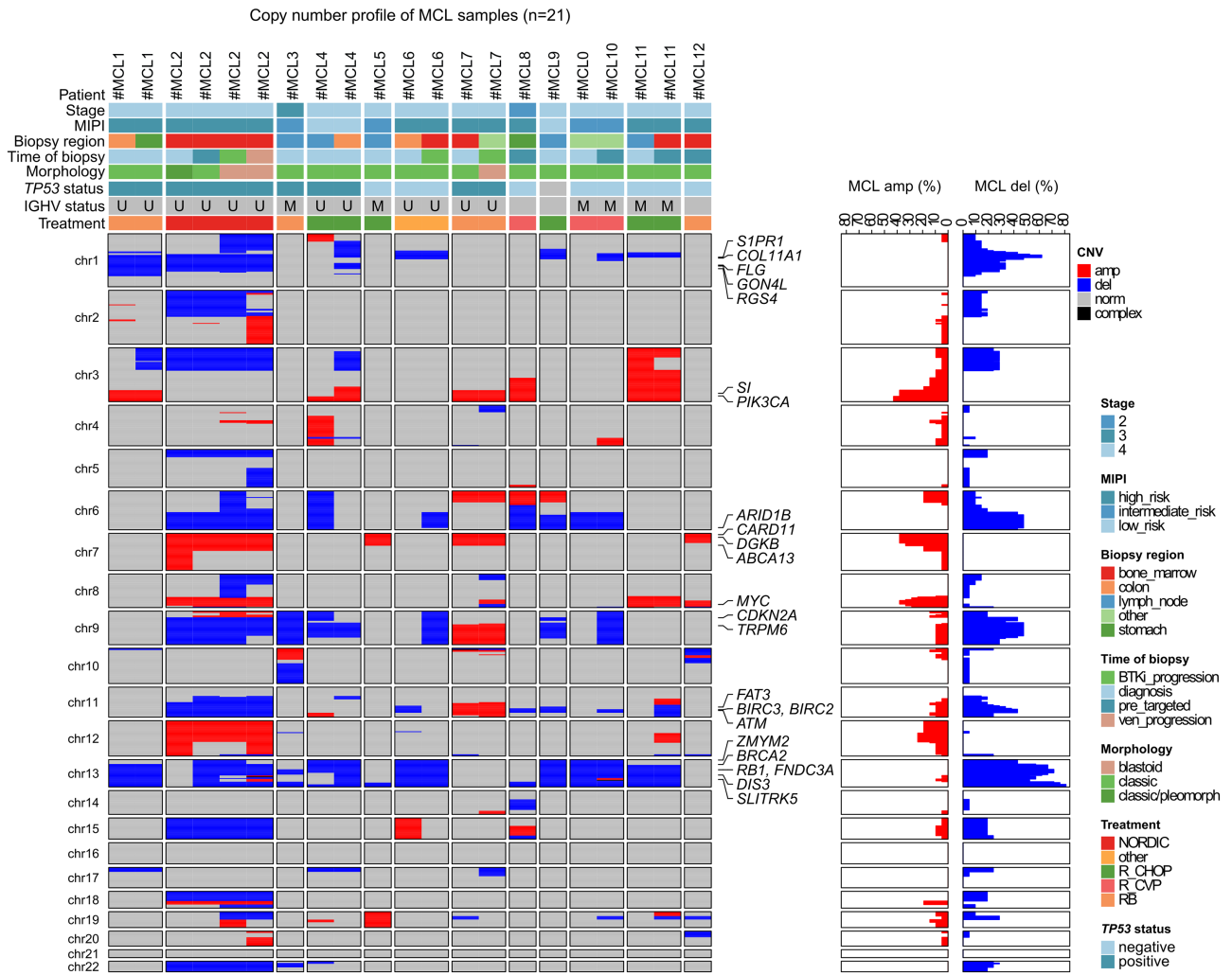


**Figure 2.** Copy number profile of all MCL samples analyzed in the study. The top part of the figure illustrates clinicopathological findings connected with the patients/samples. The patient's disease stage, MIPI score, *TP53* status, IGHV status, and treatment information refer to the patient, while information regarding the biopsy region, time of biopsy, and morphology apply to the sample. Genes in regions harboring a CNA in at least 35% of the samples are displayed on the right side of the heatmap.

Deletions affecting cytobands 9q34.3 and 22q11.23 were observed in two of three nonresponder patients spanning the coding regions of *NOTCH1*, *TRAF2*, *BCR*, and *KIAA1671* (Table 1). Amplifications present in at least two nonresponder patients affected cytobands 7p22.2, 7p21.2, and 7p12.3 encompassing the coding regions of *CARD11*, *DGKB*, and *ABCA13*. While deletions on chromosome 13q emerged with similar frequency in both early and late progressor BTKi patients, the ratio substantially varied regarding venetoclax responsiveness. Nonresponsive patients displayed an absence of arm-level deletion of 13q, whereas this alteration was most prevalent among responders (six out of nine). Despite deletions being common, amplifications were rather infrequent, occurring in three out of nine instances and impacting a significant section of the long arm of chromosome 3 (3q25.31–3q29), including the coding region of *PIK3CA*.

### Evolution of copy number profile of MCL during targeted therapy

Serial tissue samples were collected from five patients treated with BTKi and venetoclax sequentially. In two cases (patients MCL10 and MCL11), diagnostic and pretargeted samples (collected after chemotherapy but before the initiation of targeted treatment) were available. In two other patients (patients MCL6 and MCL7), samples were available from the time of diagnosis and BTKi relapse. Additionally, in one case (MCL2), sequential samples from the time of diagnosis, first relapse on chemo-immunotherapy, relapse on ibrutinib, and relapse on venetoclax were available (Figure 3). Comparison of the number of CNAs between samples collected before and after treatment initiation ( $n = 21$ ) showed significant differences, with samples collected after treatment harboring a higher number of CNAs ( $p = 0.039$ ; Wilcoxon test; data not

Table 1. Molecular changes detected in ibrutinib and venetoclax resistance.

|  | Patient ID | Cytoband affected | Deletion/ amplification      | Affected gene(s)*                       | Time of sampling  |
|--|------------|-------------------|------------------------------|---|---|
| Most common changes in BTKi early progressors        | 2,6,11     | 1p21.2            | Del                          | <i>S1PR1</i>                            | Samples obtained before start of treatment initiation with targeted therapy |
|  | 2,3,7      | 9q34.3            | Del(2), amp (1) <sup>†</sup> | <i>NOTCH1, TRAF2</i>                    |   |
|  | 2,6,7      | 11q14.2           | Del(2), amp (1) <sup>†</sup> | <i>EED</i>                              |   |
|  | 2,6,7      | 11q14.3           | Del(2), amp (1) <sup>†</sup> | <i>FAT3</i>                             |   |
|  | 2,6,7      | 11q22.2           | Del(2), amp (1) <sup>†</sup> | <i>BIRC2, BIRC3</i>                     |   |
|  | 2,6,7      | 11q22.3           | Del(2), amp (1) <sup>†</sup> | <i>ATM</i>                              |   |
|  | 3,6,11     | 13q14.2           | Del                          | <i>FNDC3A, RB1</i>                      |   |
| Most common changes in venetoclax nonresponders      | 2,3        | 9p21.3            | Del                          | <i>CDKN2A</i>                           | Samples obtained at BTKi relapse  |
|  | 2,3,7      | 9q34.3            | Del (2), amp(1) <sup>†</sup> | <i>NOTCH1, TRAF2</i>                    |   |
|  | 2,3        | 22q11.23          | Del                          | <i>BCR, KIAA1671</i>                    |   |
|  | 2,7        | 7p22.2            | Amp                          | <i>CARD11</i>                           |   |
|  | 2,7        | 7p21.2            | Amp                          | <i>DGKB</i>                             |   |
|  | 2,7        | 7p12.3            | Amp                          | <i>ABCA13</i>                           |   |
| Novel changes occurring at BTKi relapse <sup>‡</sup> | 2,7        | 8p12–8p23.2       | Del                          | <i>DLC1</i>                             | Samples obtained at venetoclax relapse                                      |
| Novel changes occurring at venetoclax relapse        | 2          | 2q14.2–37.3       | Amp                          | <i>PPIG, TTN, CASP8, SP140</i>          |   |
|  |            | 5q14.3–35.3       | Del                          | <i>APC, EGR1, PCDHB2, PDGFRB, CHSY3</i> |   |
|  |            | 20q11.21–13.33    | Amp                          | <i>CCM2L, SAMHD1, GNAS</i>              |   |

\*Genes with potential role in MCL pathogenesis or resistance are included.

<sup>†</sup>Amplification detected exclusively in patient MCL7 treated with acalabrutinib.

<sup>‡</sup>CNAs occurring in at least two of three relapsed samples.

shown). Considering the proportion of genomes altered by CNAs, no significant differences were observed; however, a trend toward more altered genomes at progression was clearly noteworthy ( $p = 0.055$ ; Wilcoxon test; data not shown).

During chemo-immunotherapy, copy number profiles of serial samples ( $n = 3$  pairs) showed overlapping alterations with new variants emerging and existing alterations diminishing at relapse. Novel arm-level alterations showed deleterious dominance, while arm-level amplification appeared in only one case. Although CNAs were usually considered stable during the disease course, loss of preexisting arm-level amplifications were identified in two samples, affecting the short arm of chromosome 3 (MCL11) and the long arms of chromosomes 7 and 12 (MCL2) (supplementary material, Figure S1).

Comparison of samples obtained at the time of diagnosis and BTKi relapse (three pairs) revealed new variants, predominantly deletions, emerging at relapse. While no cytobands were universally affected in all relapsed samples, a small number of cytobands were impacted in two samples, covering the coding region of genes previously associated with MCL. Novel loss of 8p12–8p23.2 was identified in two out of three relapsed samples containing the coding region of *DLC1*, a crucial element of cell adhesion reported to be significantly mutated in MCL (Table 1).

#### Temporal analysis of clonal evolution in double-resistant patient undergoing morphological shift

Patient MCL2 presented with pancytopenia and a diffuse lymphoid infiltration positive for CD20 and cyclin-D1, confirming the diagnosis of MCL (supplementary material, Figures S2 and S3). Treatment was initiated within a

month according to the NORDIC protocol. After 39 months, the patient developed neutropenia and anemia associated with worsening lymphadenopathy, requiring salvage treatment with ibrutinib. Four months later, pancytopenia developed, and a bone marrow biopsy revealed lymphoid infiltration with blastoid components (Figure 3, supplementary material, Figures S2 and S3). The patient was administered venetoclax therapy. Five months after initiation of venetoclax, pancytopenia reemerged, and the patient died 6 months later due to MCL progression.

The patient displayed a complex, branching clonal evolution, with certain alterations remaining persistent, while others emerged and receded with each relapse and treatment modification (Figure 3). In the respective diagnostic samples, lcWGS revealed a complex genomic pattern, with multiple CNAs present that persisted throughout the disease course: del(1)(p12p22.2), del(1)(q11–24.3), del(2)(p25.1–25.3), del(2)(q12.1–13), del(3)(p11.1–26.3), del(5)(p13.3–15.33), del(6)(q16.1–27), amp(7)(p22.3–q11.23), amp(8)(q22.3–24.22), del(9)(p21.3–q31.2), del(11)(q13.3–25), amp(12)(p13.33–q21.2), del(15)(q11.2–26.3), del(18)(p11.32–q21.1), amp(18)(q21.2–21.33), and del(22)(q11.1–13.33) (Figure 3). At first relapse on chemo-immunotherapy, existing amplifications affecting the long arms of chromosomes 7 and 12 diminished, whereas novel gains affecting the short arm of chromosome 9 (9p24.2–24.3) and (9p22.1–22.2) were detected. Like the majority of novel CNAs, these amplifications persisted throughout the remaining clinical course. In addition to amplifications, novel large deletions affecting chromosomes 11 and 13 were detected: del(11)(q11–13.2) and del(13)(q12.11–34). Along with the morphological switch, novel deletions and amplifications emerged at the time of ibrutinib relapse and were also present in the subsequent sample obtained at venetoclax

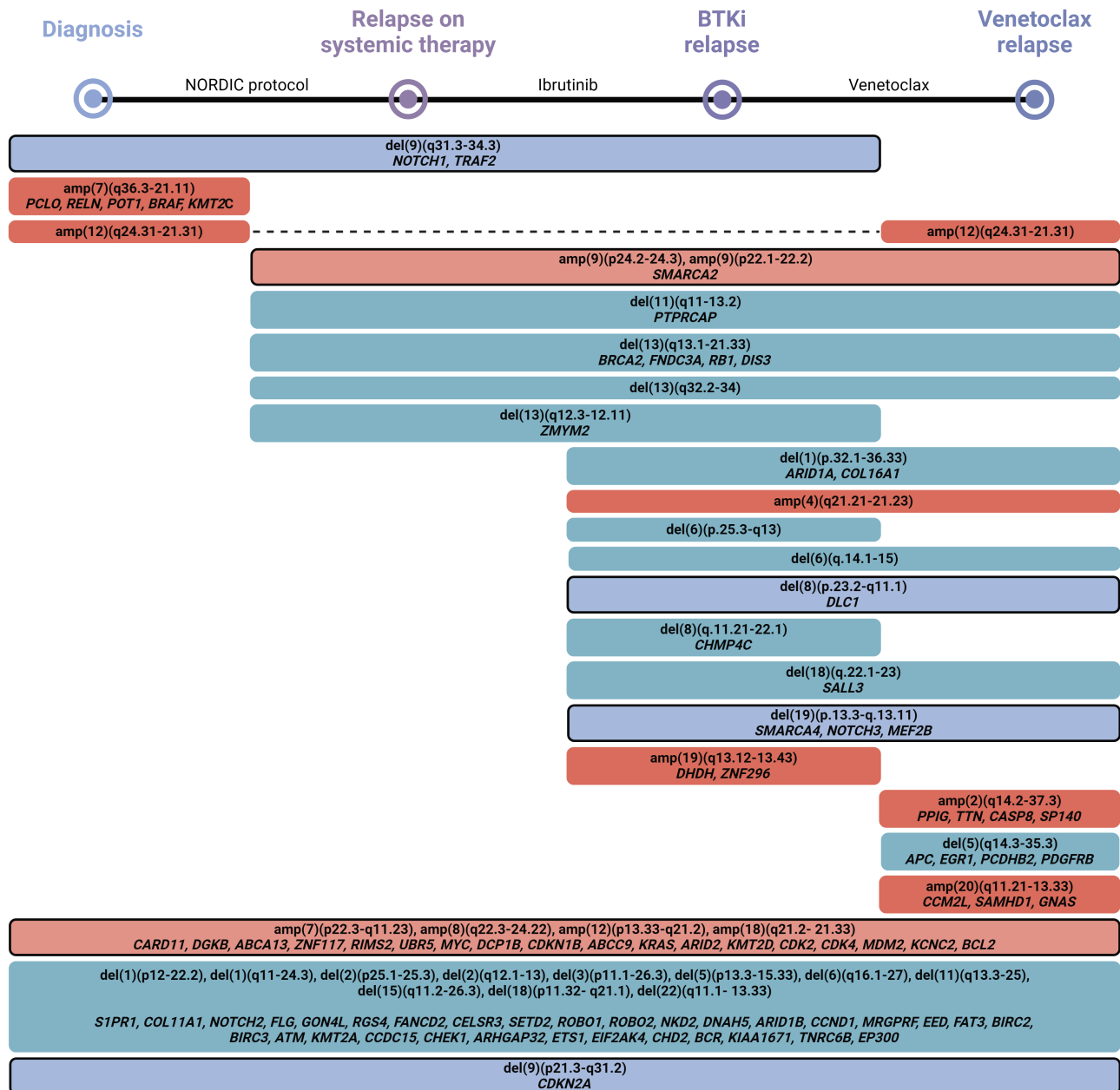


**Figure 3.** Copy number profile of patient MCL2. Red bars indicate the presence of an amplification, whereas blue bars represent a deletion. The length of the respective bar indicates the presence of CNAs relative to the time of diagnosis/first relapse/BTKi relapse or venetoclax relapse. Genes located within the corresponding cytobands are displayed at the lower section of each bar. Bordered bars indicate chromosomal regions containing potentially important genes in the development of therapy resistance such as *CARD11*, *CDKN2A*, or *DLC1*. Created in [BioRender.com](#).

relapse. Among these CNAs, deletions affecting the coding regions of *SMARCA4* [del(19)(p13.3–q13.11)], a major element in the SWI-SNF chromatin remodeling complex, as well as *DLC1* [del(8)(p23.2–q11.1)] were identified (Figure 3).

In the last sample from patient MCL2, lcWGS revealed novel CNAs emerging, with new amplifications being the dominant form of alteration. These new gains included the amplification of the long arm of chromosome 2, reoccurrence of amp(12)(q21.31–24.31) present in the initial diagnostic sample, and gain of the long arm of chromosome 20. In addition to amplifications, a novel deletion affecting the long arm of chromosome 5 del(5)(q14.3–35.3) was identified (Table 1). In addition to the

appearance of novel CNAs, venetoclax treatment successfully eliminated major deletions present in the diagnostic and previous relapsed samples, respectively: del(2)(p24.1–13.1) and del(9)(q31.3–34.3). Similarly, several deletions acquired during chemo-immunotherapy or ibrutinib treatment were eliminated during BCL2 inhibitor therapy (Figure 3).

## Discussion

Despite the high efficacy of targeted agents such as BTKi or venetoclax in the treatment of refractory/

relapsed MCL, resistance develops in most cases. Since the OS and duration of response gradually decrease with the number of therapy lines, there is a high clinical demand for the identification of prognostic and predictive biomarkers in this patient group. Although the genetic profile of MCL is becoming increasingly well defined, there is a limited amount of data available on the molecular basis of resistance mechanisms, particularly in the context of venetoclax resistance.

In our study, we explored the genome-wide copy number profiles of 12 patients treated sequentially with BTKi and venetoclax by performing lcWGS on 21 samples to understand potential resistance mechanisms to novel treatment modalities, as well as to dissect the clonal dynamics during therapy. LcWGS revealed a complex copy number profile, with novel alterations impacting critical components of pathways previously identified as potentially associated with resistance to targeted therapies.

In the early progressor group receiving BTKi treatment, the most frequently affected cytobands included 1p21.2, 9q34.3, 11q14.2, 11q14.3, 11q22.2, 11q22.3, and 13q14.2 regions. These cytobands contain the coding sequences of genes linked to the noncanonical NF- $\kappa$ B pathway, specifically *TRAF2*, *BIRC2*, and *BIRC3*. In addition, cytoband 9q34.3 (*TRAF2*) was unaffected in all late progressor cases, and 11q22.2 (*BIRC2*, *BIRC3*) was only affected in two out of seven cases. Currently, it is hypothesized that the involvement of the noncanonical NF- $\kappa$ B pathway affects the development of resistance to ibrutinib. Rahal *et al* demonstrated that crucial genes of the noncanonical NF- $\kappa$ B pathway, including *TRAF2* and *BIRC3*, were found to be mutated in resistant MCL cells [17]. Cytobands encompassing the aforementioned coding region of genes were affected in three out of five early progressor cases to BTKi, although both amplifications and deletions were observed (two deletions, one amplification). Notably, amplification of both *TRAF2* and *BIRC3* was only identified in patient MCL7, who received acalabrutinib, while deletions were found in cases that were resistant to ibrutinib, consistent with earlier findings. Our data offer further evidence concerning the involvement of the alternative NF- $\kappa$ B pathway in promoting reduced sensitivity to ibrutinib, as well as novel insights into the role of CNAs in this context. Furthermore, we compared sequential samples from the time of diagnosis and BTKi relapse in three cases. Although no cytobands were universally affected in all relapsed samples, novel loss of 8p12–8p23.2 was identified in two out of three relapsed samples containing the coding region of *DLC1*, a crucial element of cell adhesion reported to be significantly mutated in MCL [13]. This gene acts as a tumor suppressor in several frequent cancers, including prostate, lung, colorectal, and breast cancers. Although *DLC1* was described as ‘significantly mutated’ in MCL (Zhang *et al*) [13], its potential impact on BTKi resistance has never been reported previously.

Although the dismal prognosis of venetoclax-resistant patients is well known, there are only two studies reporting data regarding the genetic background of this

phenomenon. Agrawal *et al* performed whole exome sequencing on 24 patients treated with ibrutinib and venetoclax (AIM clinical cohort) [20]. Despite the limited sample size, the baseline genomic characterization allowed a clear distinction between responder and nonresponder cases based on the mutational profiles, which were characterized by the exclusive presence of *SMARCA4*, *CCND1*, *TRAF2*, and *NOTCH1* mutations, along with the deletion of chromosome 9p21.1–24.3 in the nonresponsive cohort [20]. The deleted region (9p21.1–24.3) encompasses potential oncogenes and tumor suppressors including *CDKN2A/B*. Performing *in vitro* analyses, Agrawal *et al* concluded that loss of *CDKN2A/B* could facilitate resistance to ibrutinib and venetoclax in the context of impaired SWI/SNF activity, like loss of *SMARCA4* [20]. Zhao *et al* provided the first genomic information about clonal dynamics in previously treated R/R venetoclax-resistant MCL by analyzing five paired samples by whole exome sequencing [10]. As with patients treated with venetoclax and ibrutinib combination, the presence of *SMARCA4* mutations at the time of relapse was reported, along with other alterations in the *TP53*, *CELSR3*, *CCND1*, and *KMT2D* genes [10].

In our cohort, two out of three patients experiencing early progression on venetoclax experienced loss of 9p21.3 encompassing the coding region of *CDKN2A*, a well-known adverse prognostic biomarker, reported to potentially promote venetoclax resistance in MCL [20]. Patient MCL2, harboring four sequential samples, displayed a deletion of 9p21.3 consistently across the disease course alongside the deletion of *SMARCA4* [del (19)(p13.3-q13.11)], identified at the point of ibrutinib relapse and maintained in the subsequent sample during venetoclax resistance. This finding further strengthens the idea that loss of *CDKN2A* may play a key role in primary venetoclax resistance. Patients with early progression on venetoclax also displayed deletions affecting the coding regions of *TRAF2/NOTCH1* (9q34.3) and amplification of *CARD11* (7p22.2). Loss-of-function mutations in *TRAF2*, along with gain-of-function mutations in *CARD11*, are causing constitutive, BCR-independent activation of NF- $\kappa$ B2 and NF- $\kappa$ B1 and have been linked to resistance to ibrutinib [17,18,21,31]. While no early progressor patient exhibited both *TRAF2/NOTCH1* deletion and *CARD11* amplification, each patient displayed at least one of these alterations, indicating constitutive activation of NF- $\kappa$ B2/NF- $\kappa$ B1. Our data indicate that the involvement of the NF- $\kappa$ B pathway may have a negative impact on the success of targeted treatments in general in MCL, rather than specifically causing resistance to BTKi therapies. In addition, our results suggest that copy number changes may have a similar impact on the constitutive activation of the pathway as point mutations.

Understanding the genetic basis of resistance mechanisms in MCL is crucial since patients who experience a relapse following targeted treatment experience unfavorable clinical outcomes. This study employed lcWGS, a cutting-edge genome-wide NGS-based technique, to

detect CNAs in multidrug-resistant MCL samples. Although we acknowledge the limitations of our study, including the limited sample size, we believe that, given the scarcity of available data, our findings contribute valuable insights into the critical issue of resistance to targeted treatment modalities.

## Acknowledgements

The authors acknowledge Stefánia Gróf, Barbara Zoé Csókási, and Szilárd Gudor (Department of Pathology and Experimental Cancer Research, Semmelweis University, Budapest, Hungary) for assisting in performing the *TP53* and immunoglobulin sequencing analyses.

The study was supported by the János Bolyai Research Scholarship program of the Hungarian Academy of Sciences (BO/00125/22); the National Research, Development, and Innovation Office, Hungary (K21-137948, FK20-134253, TKP2021-EGA-24, TKP2021-NVA-15); the European Union (Horizon Program, H2020-739593) and the new National Excellence Program of the Ministry for Culture and Innovation from the source of the National Research, Development and Innovation Fund (EKÖP-2024-114, EKÖP-2024-73); and the Lendület Program of the Hungarian Academy of Sciences (LP2024-3).

## Author contributions statement

TL, LIP, FM and CsB designed the study. TL, BB and BT performed the experiments. TL, BB, LV, BT and DA performed data analysis. IT, MP, ZsN, PR, ME, ZsM, JR, AM, PT, RSz, ÁI, AG, LIP and FM provided patient samples and/or annotations. TL and CsB wrote the paper. All authors read and critically reviewed the final version of the manuscript.

## Data availability statement

Raw sequencing data are available from the corresponding author upon reasonable request.

## References

- Kumar A, Sha F, Toure A, *et al.* Patterns of survival in patients with recurrent mantle cell lymphoma in the modern era: progressive shortening in response duration and survival after each relapse. *Blood Cancer J* 2019; **9**: 50.
- Dreyling M, Goy A, Hess G, *et al.* Long-term outcomes with ibrutinib treatment for patients with relapsed/refractory mantle cell lymphoma: a pooled analysis of 3 clinical trials with nearly 10 years of follow-up. *Hemasphere* 2022; **6**: e712.
- Rule S, Dreyling M, Goy A, *et al.* Ibrutinib for the treatment of relapsed/refractory mantle cell lymphoma: extended 3.5-year follow up from a pooled analysis. *Haematologica* 2019; **104**: e211–e214.
- Wang M, Rule S, Zinzani PL, *et al.* Long-term follow-up of acalabrutinib monotherapy in patients with relapsed/refractory mantle cell lymphoma. *Blood* 2018; **132**: 2876.
- Wang M, Rule S, Zinzani PL, *et al.* Acalabrutinib in relapsed or refractory mantle cell lymphoma (ACE-LY-004): a single-arm, multicentre, phase 2 trial. *Lancet* 2018; **391**: 659–667.
- Wang ML, Lee H, Chuang H, *et al.* Ibrutinib in combination with rituximab in relapsed or refractory mantle cell lymphoma: a single-centre, open-label, phase 2 trial. *Lancet Oncol* 2016; **17**: 48–56.
- Wang ML, Rule S, Martin P, *et al.* Targeting BTK with ibrutinib in relapsed or refractory mantle-cell lymphoma. *N Engl J Med* 2013; **369**: 507–516.
- McCulloch R, Lewis D, Crosbie N, *et al.* Ibrutinib for mantle cell lymphoma at first relapse: a United Kingdom real-world analysis of outcomes in 211 patients. *Br J Haematol* 2021; **193**: 290–298.
- Toby AE, Harriet SW, Sunil I, *et al.* Efficacy of venetoclax monotherapy in patients with relapsed, refractory mantle cell lymphoma after Bruton tyrosine kinase inhibitor therapy. *Haematologica* 2019; **104**: e68–e71.
- Zhao S, Kanagal-Shamanna R, Navsaria L, *et al.* Efficacy of venetoclax in high risk relapsed mantle cell lymphoma (MCL) - outcomes and mutation profile from venetoclax resistant MCL patients. *Am J Hematol* 2020; **95**: 623–629.
- Sawalha Y, Goyal S, Switchenko JM, *et al.* A multicenter analysis of the outcomes with venetoclax in patients with relapsed mantle cell lymphoma. *Blood Adv* 2023; **7**: 2983–2993.
- Beà S, Valdés-Mas R, Navarro A, *et al.* Landscape of somatic mutations and clonal evolution in mantle cell lymphoma. *Proc Natl Acad Sci U S A* 2013; **110**: 18250–18255.
- Zhang J, Jima D, Moffitt AB, *et al.* The genomic landscape of mantle cell lymphoma is related to the epigenetically determined chromatin state of normal B cells. *Blood* 2014; **123**: 2988–2996.
- Jain P, Kanagal-Shamanna R, Zhang S, *et al.* Long-term outcomes and mutation profiling of patients with mantle cell lymphoma (MCL) who discontinued ibrutinib. *Br J Haematol* 2018; **183**: 578–587.
- Kotmayer L, László T, Mikala G, *et al.* Landscape of BCL2 resistance mutations in a real-world cohort of patients with relapsed/refractory chronic lymphocytic leukemia treated with venetoclax. *Int J Mol Sci* 2023; **24**: 5802.
- Bödör C, Kotmayer L, László T, *et al.* Screening and monitoring of the BTK(C481S) mutation in a real-world cohort of patients with relapsed/refractory chronic lymphocytic leukaemia during ibrutinib therapy. *Br J Haematol* 2021; **194**: 355–364.
- Rahal R, Frick M, Romero R, *et al.* Pharmacological and genomic profiling identifies NF- $\kappa$ B-targeted treatment strategies for mantle cell lymphoma. *Nat Med* 2014; **20**: 87–92.
- Wu C, de Miranda NF, Chen L, *et al.* Genetic heterogeneity in primary and relapsed mantle cell lymphomas: impact of recurrent CARD11 mutations. *Oncotarget* 2016; **7**: 38180–38190.
- Zhang L, Yao Y, Zhang S, *et al.* Metabolic reprogramming toward oxidative phosphorylation identifies a therapeutic target for mantle cell lymphoma. *Sci Transl Med* 2019; **11**: eaau1167.
- Agarwal R, Chan YC, Tam CS, *et al.* Dynamic molecular monitoring reveals that SWI-SNF mutations mediate resistance to ibrutinib plus venetoclax in mantle cell lymphoma. *Nat Med* 2019; **25**: 119–129.
- Decombis S, Bellanger C, Bris Y, *et al.* CARD11 gain of function upregulates BCL2A1 expression and promotes resistance to targeted therapies combination in B-cell lymphoma. *Blood* 2023; **142**: 1543–1555.
- Scheinin I, Sie D, Bengtsson H, *et al.* DNA copy number analysis of fresh and formalin-fixed specimens by shallow whole-genome

- sequencing with identification and exclusion of problematic regions in the genome assembly. *Genome Res* 2014; **24**: 2022–2032.
23. Carbone PP, Kaplan HS, Musshoff K, *et al*. Report of the committee on Hodgkin's disease staging classification. *Cancer Res* 1971; **31**: 1860–1861.
  24. Cheson BD, Ansell S, Schwartz L, *et al*. Refinement of the Lugano classification lymphoma response criteria in the era of immunomodulatory therapy. *Blood* 2016; **128**: 2489–2496.
  25. László T, Kotmayer L, Fésüs V, *et al*. Low-burden TP53 mutations represent frequent genetic events in CLL with an increased risk for treatment initiation. *J Pathol Clin Res* 2024; **10**: e351.
  26. Agathangelidis A, Sutton LA, Hadzidimitriou A, *et al*. Immunoglobulin gene sequence analysis in chronic lymphocytic leukemia: from patient material to sequence interpretation. *J Vis Exp* 2018; **26**: e57787.
  27. Rosenquist R, Ghia P, Hadzidimitriou A, *et al*. Immunoglobulin gene sequence analysis in chronic lymphocytic leukemia: updated ERIC recommendations. *Leukemia* 2017; **31**: 1477–1481.
  28. van Beers EH, Joosse SA, Ligtenberg MJ, *et al*. A multiplex PCR predictor for aCGH success of FFPE samples. *Br J Cancer* 2006; **94**: 333–337.
  29. Bártai B, Kiss L, Varga L, *et al*. Profiling of copy number alterations using low-coverage whole-genome sequencing informs differential diagnosis and prognosis in primary cutaneous follicle center lymphoma. *Mod Pathol* 2024; **37**: 100465.
  30. Andersen NS, Pedersen L, Elonen E, *et al*. Primary treatment with autologous stem cell transplantation in mantle cell lymphoma: outcome related to remission pretransplant. *Eur J Haematol* 2003; **71**: 73–80.
  31. Lenz G, Davis RE, Ngo VN, *et al*. Oncogenic CARD11 mutations in human diffuse large B cell lymphoma. *Science* 2008; **319**: 1676–1679.

### SUPPLEMENTARY MATERIAL ONLINE

**Figure S1.** Frequency histogram of copy number variations at cytoband and arm resolution

**Figure S2.** Histopathological characteristics of patient MCL2

**Figure S3.** Morphological and detailed molecular characteristics of patient MCL2

**Table S1.** Clinical characteristics

**Table S2.** Clinicopathological characteristics

**Table S3.** Copy number alterations